ORIGINAL ARTICLE

Syringaresinol Resisted Sepsis-Induced Acute Lung Injury by Suppressing Pyroptosis *Via* the Oestrogen Receptor-β Signalling Pathway

Yuzhen Zhuo[1], Lei Yang[1] , Dihua Li[1] , Lanqiu Zhang[1] , Qi Zhang[1] , Shukun Zhang[1] , Caixia Li[1] , Lihua Cui[1] , Jian Hao[2] , Jiarui Li[3,5] and Ximo Wang[1,4,5]

Abstract— Acute lung injury (ALI) is a common lung disease characterized by severe acute inflammatory lung injury in patients with sepsis. Syringaresinol (SYR) has been reported to have anti-apoptotic and anti-inflammatory effects, but whether it could prevent pyroptosis to improve sepsis-induced ALI remains unclear. The purpose of this work was to examine the impact of SYR on sepsis-induced ALI and investigate the underlying mechanisms. The ALI model was induced by caecal ligation and puncture (CLP) in C57BL/6 mice, structural damage in the lung tissues was determined using haematoxylin and eosin (HE) staining, and the levels of related inflammatory cytokines and macrophage polarization were examined by enzyme-linked immunosorbent assays (ELISAs) and flow cytometry, respectively. The activation of the NLRP3 inflammasome and the protein levels of TLR4, NF-κB and MAPKs was measured by western blotting. The results demonstrated that SYR pretreatment significantly reduced lung tissue histological damage, inhibited the production of proinflammatory cytokines and albumin in bronchoalveolar lavage fluid (BALF), and decreased myeloperoxidase (MPO) levels, thereby alleviating lung tissue injury. Meanwhile, septic mice treated with SYR displayed a higher survival rate and lower percentage of M1 macrophages in the BALF and spleen than septic mice. In addition, lung tissues from the CLP + SYR group exhibited downregulated protein expression of NLRP3, ASC, GSDMD caspase-1 p20 and TLR4, along with decreased phosphorylated levels of NF-κB, ERK, JNK and P38, indicating that SYR administration effectively prevented CLP-induced pyroptosis in the lung. SYR also suppressed LPS-induced pyroptosis in RAW 264.7 cells

Yuzhen Zhuo and Lei Yang contributed equally to this work.

___

[1]Tianjin Institute of Acute Abdominal Diseases of Integrated Traditional Chinese and Western Medicine, Tianjin 300100, China

[2]Department of Orthopaedics, Shenzhen Pingle Orthopaedics Hospital, Shenzhen 518010, China

[3]Department of Nephrology, Tianjin Nankai Hospital, Tianjin 300100, China

[4]Tianjin Key Laboratory of Acute Abdomen Disease Associated Organ Injury and ITCWM Repair, Institute of Integrative Medicine for Acute Abdominal Diseases, Integrated Chinese and Western Medicine Hospital, Tianjin University, Tianjin 300100, China

[5]To whom correspondence should be addressed at Tianjin Institute of Acute Abdominal Diseases of Integrated Traditional Chinese and Western Medicine, Tianjin, 300100, China. Email: wangximonkyy@126.com and Department of Nephrology, Tianjin Nankai Hospital, Tianjin, 300100, China. Email: 13821359282@163.com

by inhibiting the activation of the NLRP3 inflammasome, which was abolished by an oestrogen receptor-β (ERβ) antagonist (PHTPP). In conclusion, SYR exerted protective effects on CLP-induced ALI via the oestrogen receptor-β signalling pathway.

KEY WORDS: Sepsis; Acute lung injury; Syringaresinol; Pyroptosis; Oestrogen receptor-β.

INTRODUCTION

Acute lung injury (ALI) is a common life-threatening respiratory system disease around the world that is induced by various external and internal factors, such as sepsis, trauma, bacterial infection and hyperventilation [1, 2]. ALI is characterized by inflammatory cell infiltration and disruption of the alveolar-capillary interface, which can trigger pulmonary interstitial oedema, refractory hypoxemia and progressive dyspnoea, ultimately leading to death [3, 4]. The major reason for the high mortality of ALI is uncontrolled lung inflammation [5]; therefore, inhibition of excessive inflammatory response in the lung is considered to be a potential strategy for ALI. Despite great progress in illustrating the pathophysiology and treatments for ALI/ARDS, there is no effective pharmacologic treatment so far, and the morbidity and mortality of ALI in the intensive care unit remain high [6]. Hence, it is of great significance to explore new effective treatments for ALI and to reveal the underlying molecular mechanisms.

According to previous reports, activating NLRP3 inflammasomes induces macrophage pyroptosis in a mouse model of acute lung injury [7]. The NLRP3 inflammasome is recognized as a host defence mechanism to clear microbial infection and plays important roles in the response to infectious diseases. However, excessive activation of the NLRP3 inflammasome is harmful to the host and contributes to uncontrolled inflammatory reactions, the progression of tissue damage and multiple organ dysfunction [8]. Studies have found that the NLRP3 inflammasome is associated with the progression of ALI/ARDS, and attenuating the excessive activation of the NLRP3 inflammasome effectively protects against ALI/ARDS [9–11]. The NLRP3 inflammasome is composed of the central protein NLRP3, the adaptor protein ASC (apoptosis-associated speck-like protein) and the effector protein caspase-1 [12]. As the key component, NLRP3 can recognize pathogen-associated molecular patterns (PAMPs), such as nigericin or damage-associated molecular patterns (DAMPs), such as ATP. Activated NLRP3 causes recruitment of the adaptor ASC and the autocatalytic activation of caspase-1. Caspase-1 then catalyses the precursor forms

of IL-18, IL-1β and gasdermin D (GSDMD, a member of the gasdermin family) into their active forms [13–15], which further promotes the production of various proinflammatory cytokines, such as tumour necrosis factor-α (TNF-α), IL-6, inducible nitric oxide synthase (iNOS) and cyclooxygenase-2 (COX2), eventually leading to inflammatory disorders [16, 17]. After stimulation, activated nuclear factor-κB (NF-κB) upregulates a variety of proinflammatory cytokines, including IL-1β, IL-6 and TNF-α, and IL-1β is a key player in the activation of NLRP3 inflammasomes. Toll-like receptor 4 (TLR4) enhances the expression levels of inflammatory cytokines by regulating the NF-κB signalling pathway and activating the NLRP3 inflammasome [18]. Mitogen-activated protein kinases (MAPKs), which are associated with the production of proinflammatory cytokines, have also been found to play a crucial role in inflammatory responses [19, 20].

Over the past few decades, studies have shown an increasing demand for natural products due to their extensive bioactivities, low toxicity, low cost and few adverse effects in humans [21]. (+)-Syringaresinol (SYG) is a phytochemical constituent of lignan formed from two sinapyl alcohol units linked via a β–β linkage, which can be found in various cereals and medicinal plants, such as the cortex, Amelia and flax seed, *Sargentodoxa cuneata*, Panax ginseng berries and *Rubia philippinensis* [22]. In our work, SYG was isolated from *Sargentodoxa cuneata*, which is a well-known traditional Chinese medicine for treating acute appendicitis, intestinal inflammation and ulcer rheumatoid arthritis. SYG has been reported to possess various biological activities. SYG exhibits antioxidant pharmacological properties in copper/zinc superoxide dismutase-deficient mice, which reversed age-dependent skin atrophy and oxidative damage by regulating the FoxO3-matrix metalloproteinase-2 axis [23]. A recent study showed that SYG exerts anti-photoaging properties against UVA-induced skin ageing by suppressing MAPK/AP-1 signalling in HaCaT keratinocytes and dermal fibroblasts [24]. SYG possesses anti-inflammatory activities via downregulation of NF-κB protein expression as well as the mRNA levels of iNOS, COX-2, TNF-α, IL-1β and

IL-6 in vitro and in vivo [25]. It has also been reported that SYG, as a new neuromodulating agent, suppresses excitatory synaptic transmission by modulating presynaptic transmitter release [26]. In a previous study, we identified that SYG protects against type 1 diabetic cardiomyopathy by inhibiting inflammation, fibrosis and oxidative stress [27]. In addition, we have shown that SYG suppresses the Akt and NF-κB signalling pathways in LPS-induced RAW 264.7 macrophages [28]. However, the pharmacological effects of SYG on ALI induced by CLP are unknown. Therefore, in the current study, we aimed to investigate the protective effects of SYG against CLP-induced ALI and its role in modulating the NLRP3 inflammasome and NF-κB/TLR4/MAPK signalling pathways.

MATERIALS AND METHODS

Drug and Reagents

SYG was isolated from *Sargentodoxa cuneata* by our group as previously described, dissolved in dimethyl sulfoxide (DMSO) as a 100-mM stock solution and diluted with physiological saline [28]. The chemical structure of SYG was characterized using NMR spectroscopy analysis, and the purity of the isolated SYG was > 98% by normalization of the peak areas by HPLC (Fig. 1A). Protein extraction reagent was purchased from Wuhan Boster Biological Technology, Ltd. (Wuhan, China). Protein concentrations were detected using the BCA protein assay kit, and the reagent kit was supplied by Thermo Scientific (Thermo Scientific, Waltham, MA,

USA). Antibodies for GAPDH, NF-κB, p-NF-κB, EKR, p-ERK, p38, p-p38, JNK, p-JNK, TLR4, Gasdermin D, ASC and NLRP3 were purchased from Cell Signalling Technology (Boston, MA, USA). Rabbit polyclonal anticaspase 1 p20 was purchased from Abcam (Cambridge, MA, USA). APC-anti-F4/80, FITC-anti-CD11b and PE-Cy7-anti-MHCII were purchased from Invitrogen (Carlsbad, CA, USA). ELISA kits for detecting murine tumour necrosis factor-α (TNF-α), interleukin-1β (IL-1β), and interleukin-6 (IL-6) were purchased from R&D Systems (Minneapolis, MN, USA).

CLP Model and Experimental Protocol

An animal model of polymicrobial sepsis was induced by caecal ligation and puncture (CLP) as previously described [29]. We purchased C57BL/6 male mice (6–8 weeks old) from Beijing Vital River Laboratory Animal Technology Co., Ltd., (Beijing, China) and kept them in a temperature-controlled room (21–23 °C) with a 12-h light/dark cycle. The mice were allowed free access to food and water for at least 1 week to acclimatize before the experiment. All animal experiments were approved by the Medicine Ethical Committee of Tianjin Nankai Hospital and conformed to all of the rules and regulations assigned by that committee. In brief, 6- to 8-week-old C57BL/6 mice were randomly divided into three groups ($n = 5$ per group): the sham-operated group (SO), caecal ligation and puncture model group (CLP) and CLP syringaresinol group (syringaresinol). Before CLP, the syringaresinol group was administered syringaresinol (50 mg/kg body
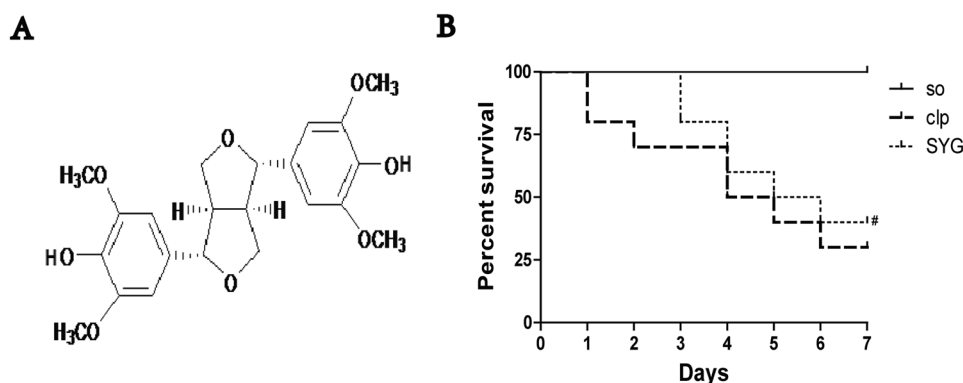

Fig. 1 Effect of SYG on the survival rate of sepsis in CLP mice. (**A**) SYG chemical structure. (**B**) SYG improves the survival rate of CLP-induced ALI mice ($n = 10$). Compared with the CLP group, the mean survival time of the SYG group was significantly increased during the 7-day observation period. #$P < 0.05$ compared with CLP groups.

weight) by gavage, and the CLP group was administered the same volume of vehicle (PBS). The SO mice were defined as normal, with only laparotomy performed but neither ligated nor punctured. Twenty-four hours after induction of CLP, the mice were anesthetized. Lung and bronchoalveolar lavage fluid (BALF) samples were collected for subsequent analysis.

Cell Culture and Stimulation

We purchased RAW 264.7 cells from the American Type Culture Collection (Manassas, VA, USA). Cells were cultured at 37 °C and 5% CO_2 in RPMI 1640 medium supplemented with 10% (v/v) FBS, 100-U/ml streptomycin, and 100-U/ml penicillin. Cells were seeded in six-well plates cultured to near-complete confluency and then preincubated with syringaresinol (100 μmol/l) for 2 h before LPS (100 ng/ml) + ATP (2.5 μM) stimulation. After the addition of syringaresinol, cells were treated with LPS + ATP for 4 h and then harvested for further experiments.

Survival Analysis

We investigated the effects of syringaresinol on mouse survival, and 30 mice were randomly divided into three groups ($n = 10$ per group). The CLP and syringaresinol groups were treated with vehicle and syringaresinol, respectively. After sham or CLP operation, the mice were observed every 24 h for 7 days, and dead mice were recorded. Survival curves were plotted.

Histological and Biochemical Analysis

The left lung was fixed with 10% formaldehyde for 24 h, dehydrated in a graded ethanol series, embedded in paraffin and sectioned into 4-μm slices. Then, the slices were stained with haematoxylin and eosin (H&E) to measure inflammatory cell infiltration. We assessed the severity of lung tissue injury according to criteria [30], and pathologists were blinded to the identification of three groups using optical microscopy.

Enzyme-Linked Immunosorbent Assay

At 24 h following the operation, bronchoalveolar lavage fluid (BALF) was obtained by intratracheal injection with cold PBS. IL-1β, IL-6 and TNF-α concentrations in BALF were evaluated by enzyme-linked

immunosorbent assay (ELISA) kits (R&D Systems) according to the manufacturer's instructions. The cytokine concentration was measured using a microtitre plate reader at 450-nm absorbance. The level of albumin is a signal to assess oedema in ALI, so we further examined the concentration of albumin in BALF using a mouse albumin ELISA kit (USCN Life Science Inc. Wuhan, China).

Flow Cytometry Analysis

Mice were euthanized 24 h after CLP, the BALF and spleen tissues were harvested, single spleen cells were collected as previously described [31], and the cells in the BALF were collected by centrifugation. The cells in the BALF and spleen were first resuspended in PBS and then stained with APC-anti-F4/80, FITC-anti-CD11b and PE-anti-MHCII, according to the manufacturer's recommendations. After incubation, cells were washed twice in PBS and finally suspended in 200-µl PBS for flow cytometry analysis using Novo-Cyte flow cytometry (ACEA Biosciences, Inc., CA, USA) and analysed by NovoExpress software (ACEA Biosciences, Inc.).

Quantitative Real-Time PCR

Total RNA in lung tissue and RAW 264.7 cells was extracted using a TRIzol reagent kit according to the manufacturer's instructions (Takara Bio, Tokyo, Japan). cDNA synthesis was performed using TransGen Reverse Transcription for qPCR. qPCR was performed using SYBR Green Master Mix (TransGen Biotech, Beijing, China) and a Bio-Rad IQ5 detection system. All reactions were performed in triplicate. GAPDH was used as an internal reference, and relative target gene expression was calculated using the $2 - \Delta\Delta Ct$ method. The primer sequences used in this study were as follows: IL-6 (forward primer: 5′-AGTTGCCTTCTTGGG ACTGA-3′; reverse primer: 5′-TCCACGATTTCCCAG AGAAC-3′), IL-1β (forward primer: 5′-CTATGTCTT GCCCGTGGAG-3′; reverse primer: 5′-CATCATCCC ACGAGTCACA-3′), TNF-a (forward primer: 5′-CGT CAGCCGATTTGCTATCT-3′; reverse primer: 5′-CGG ACTCCGCAAAGTCTAAG-3′); and GAPDH (forward primer: 5′-GCCTCGTCTCATAGACAAGATG-3′; reverse primer: 5′- CAGTAGACTCCACGACATAC-3′).

Western Blot Assay

We detected protein expression in lung tissue and RAW 264.7 cells using western blot assays. Total proteins in lung tissue and RAW 264.7 cells were extracted using a RIPA buffer containing a protease inhibitor and

phosphatase inhibitor, and then protein concentrations were detected using BCA protein assay kits (Thermo Fisher Scientific, MA, USA). Equal amounts of protein extracts were separated using sodium dodecyl sulfate–polyacrylamide (SDS-PAGE) gel electrophoresis and then transferred to polyvinylidene fluoride
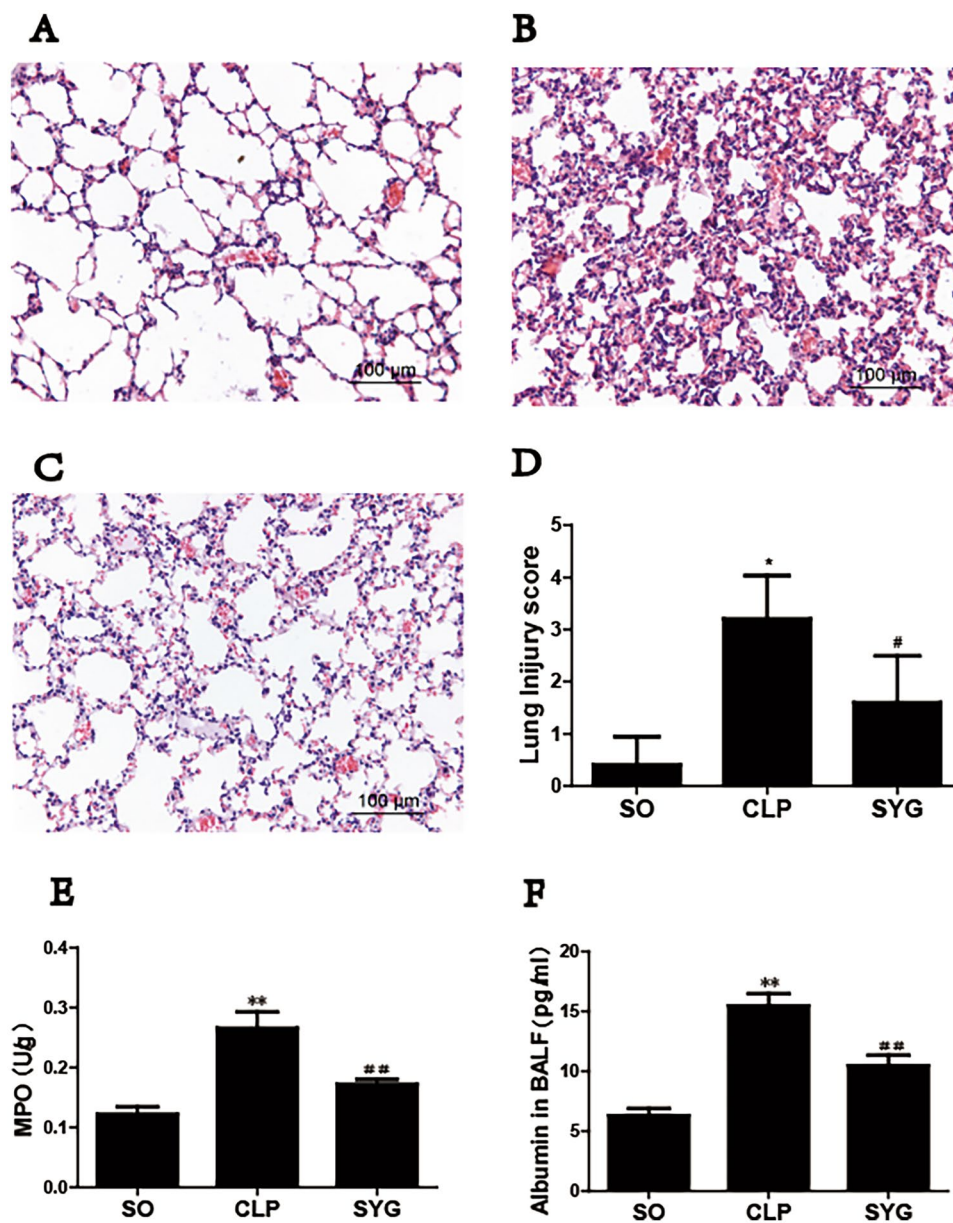

Fig. 2 SYG alleviated lung injury in mice with CLP-induced ALI. (**A–C**) Pathological changes in the lungs of mice at 24 h: (**A**) SO group, (**B**) CLP group and (**C**) SYG group. (**D**) Lung injury score at 24 h. (**E**) MPO activity in the lung tissues of ALI mice. (**F**) Albumin levels in the BALF of ALI mice. The values presented are the means $\pm SD$. ($n=5$ in each group) $*P<0.05$, $**P<0.01$ with SO group; $^{\#}P<0.05$, $^{\#\#}P<0.01$ compared with CLP group.

(PVDF) membranes (Millipore, MA, USA). The membrane was blocked with 5% (w/v) fat-free milk for 2 h at room temperature and incubated overnight at 4 °C with specific antibodies, including GAPDH, NF-κB, p-NF-κB, EKR, p-ERK, p38, p-p38, JNK, p-JNK, TLR4, ASC, NLRP3, Gasdermin D and caspase-1 p20 (1:1000). Subsequently, the membrane was incubated with horseradish peroxidase (HRP)-conjugated secondary antibodies for 2 h at room temperature. Finally, the target proteins were visualized using enhanced chemiluminescence (ECL System, Millipore, MA, USA) and quantified using Imager software (Quantity One, USA).

Statistical Methods

Statistical analysis was conducted with SPSS v17.0 (SPSS, Inc., Chicago, IL, USA) using one-way analysis of variance (ANOVA). All data are expressed as the mean $\pm$ standard deviation (*SD*), and values of $P < 0.05$ were considered statistically significant. Survival curves were analysed with the Kaplan–Meier method and compared using the log-rank test.

RESULTS

Effects of SYG on the Survival Rate in Mice with CLP-Induced ALI

To explore the therapeutic potential of SYG, we established a CLP-induced mouse ALI model to evaluate the effect of SYG on the survival rate. Log-rank test analysis of the 7-day survival curves demonstrated that the survival rate of mice was significantly improved during the 7-day observation period in the SYG group compared to the CLP group (Fig. 1B; $P < 0.05$).

SYG Alleviated Lung Injury in Mice with CLP-Induced ALI

We used haematoxylin and eosin (H&E) staining to evaluate the morphologic changes of the lung tissue in mice with CLP-induced ALI 24 h after CLP. The administration of CLP resulted in aggravated histological changes; however, the SO group was basically normal. As shown in Fig. 2A, the alveolar structure is severely damaged, with alveolar destruction, pulmonary congestion, thickening of the alveolar wall and interstitial

oedema and marked inflammatory cell infiltration in the lungs of the CLP group. In contrast, these histopathologic changes were dramatically ameliorated in the SYG groups. Accordingly, the lung injury scores were estimated and showed that SYG alleviated lung injury scores directly compared with those of the CLP groups (Fig. 2A; $P < 0.05$). MPO plays an essential role in many inflammatory diseases and reflects neutrophil infiltration. It is well known that neutrophils are the earliest recruited cells that accumulate in the lungs in the course of ALI. We used the Nanjing Jiancheng test kit to measure MPO activity in the lung tissues. As shown in Fig. 2, the levels of MPO in the SYG groups are significantly decreased compared with those of the CLP groups (Fig. 2B; $P < 0.05$). In this paper, we assessed lung oedema by detecting the levels of albumin in the BALF, which is an index of pulmonary oedema. We found that the levels of albumin in the CLP groups were significantly increased in comparison with those in the SO group, but SYG decreased the albumin level (Fig. 2C, $P < 0.05$). Taken together, these results implied that SYG could alleviate lung tissue injury in CLP-induced mice.

SYG Inhibited Inflammatory Mediators in the BALF and Lung Tissue of Septic Mice

Inflammatory cytokines play a key role in CLP-induced ALI. To determine whether SYG administration could inhibit inflammatory mediators in mice with CLP-induced ALI, we measured the concentrations of IL-1β, TNF-α and IL-6 in BALF using ELISA kits. We found that their production was evidently increased in the CLP groups, whereas these increased inflammatory cytokines could be downregulated by SYG (Fig. 3A, $P < 0.05$). We next quantified the mRNA expression levels of TNF-α, IL-6 and IL-1β in the lung tissues using real-time PCR. As expected, SYG treatment effectively reduced their gene expression (Fig. 3B). In summary, these results indicated that SYG could attenuate the inflammatory response in mice with ALI induced by CLP.

Effects of SYG on the Polarization of Macrophages to the M1 Phenotype in Mice with CLP-Induced ALI

To further investigate the effects of SYG on lung macrophages and subtypes in mice with CLP-induced ALI, we analysed macrophages and their phenotypes in BALF and spleen using flow cytometry.
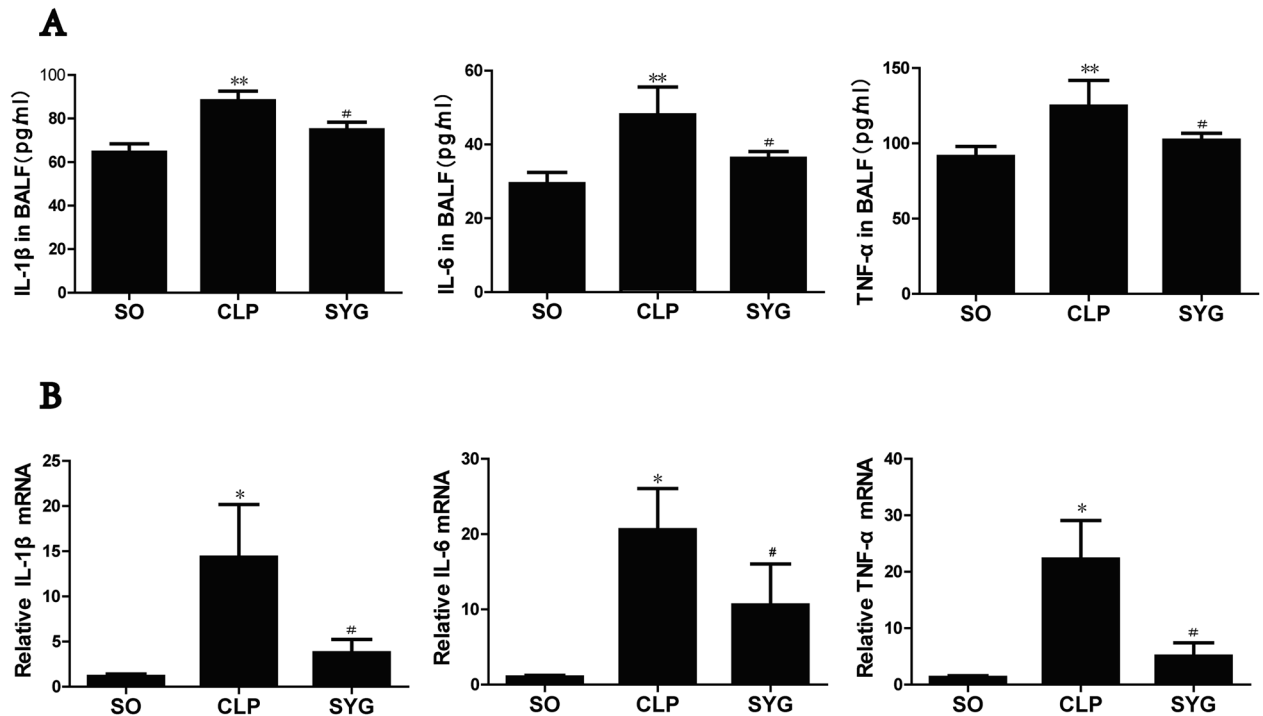
A

B

Fig. 3 SYG decreased the levels of inflammatory cytokines in BALF and lung tissues of ALI mice. (**A**) The concentrations of TNF-α, IL-6 and IL-1β in BALF. (**B**) The mRNA expression levels of TNF-α, IL-6 and IL-1β in lung tissues. Values are expressed as the mean $\pm$ SD. ($n=5$ in each group) *$P<0.05$, **$P<0.01$ compared with the SO group; #$P<0.05$ compared with the CLP group.

Classically activated macrophages (M1) were identified as MHCII + F4/80 + CD11b +. Flow cytometry analysis identified that the percentages of MHCII + F4/80 + CD11b + M1 macrophages in the spleen and BALF were increased in the CLP groups; however, SYG administration markedly decreased the percentage of M1 macrophages (Fig. 4).

Effect of SYG on NLRP3 Inflammasome-Dependent Pyroptosis in Mice with CLP-Induced ALI

To further explore the possible underlying mechanism involved in the protective effect of SYG on CLP-induced ALI, we assessed the effects of SYG on pyroptosis in mice with CLP-induced ALI. We measured the protein expression levels of NLRP3, caspase-1 p20, ASC and cleaved gasdermin D (Cle-GSDMD) in lung tissues in septic mice using western blot analysis. As shown in Fig. 5, the protein expression levels of NLRP3, ASC, Cle-GSDMD and caspase-1 p20 are markedly increased

in CLP-induced ALI compared with the SO group, whereas these levels were distinctly downregulated by SYG administration.

Effect of SYG on TLR4/NF-κB/MAPK Signalling Pathway Activation in Mice with CLP-Induced ALI

TLR4/NF-κB/MAPK signalling pathways are important intracellular signalling pathways that play a crucial role in regulating the inflammatory response in ALI. In addition, studies have found that TLR4/NF-κB/MAPK signalling pathways are involved in the activation of the NLRP3 inflammasome. Therefore, we assessed the activities of the TLR4/NF-κB/MAPK signalling pathway using western blotting in lung tissue homogenates. We discovered that the protein expression levels of TLR4 were increased and that the NF-κB and MAPK signalling pathways were activated in CLP-induced mice, while these effects were obviously reversed by SYG treatment (Fig. 6A, B).

M1 macrophages in the BALF

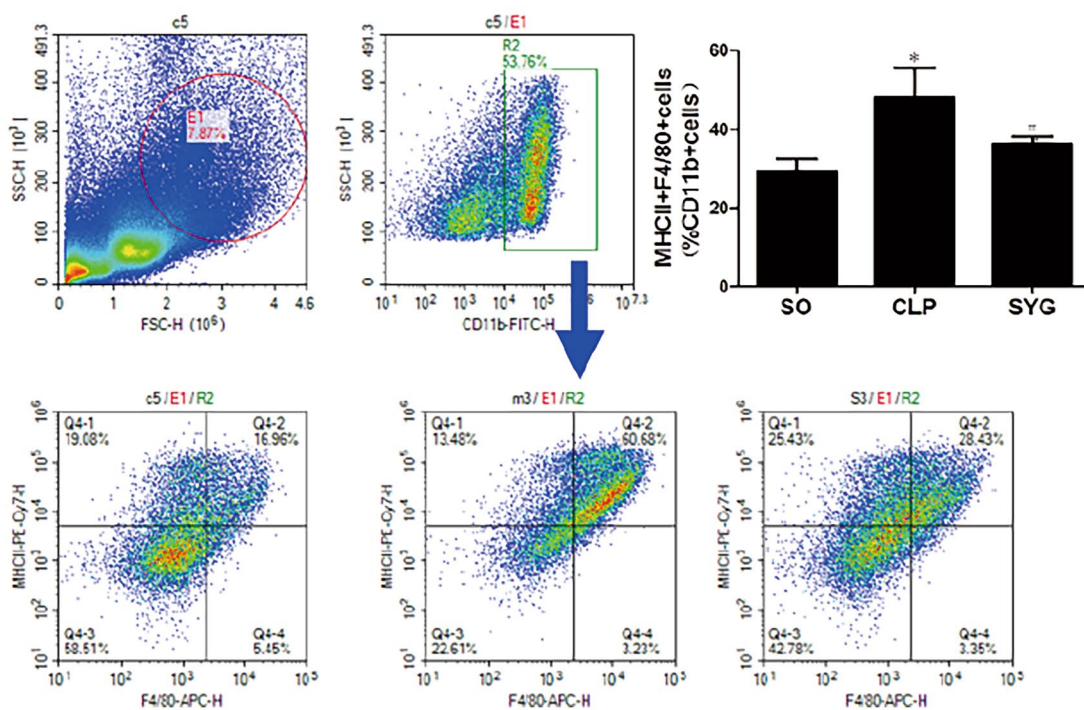SO   CLP   SYG
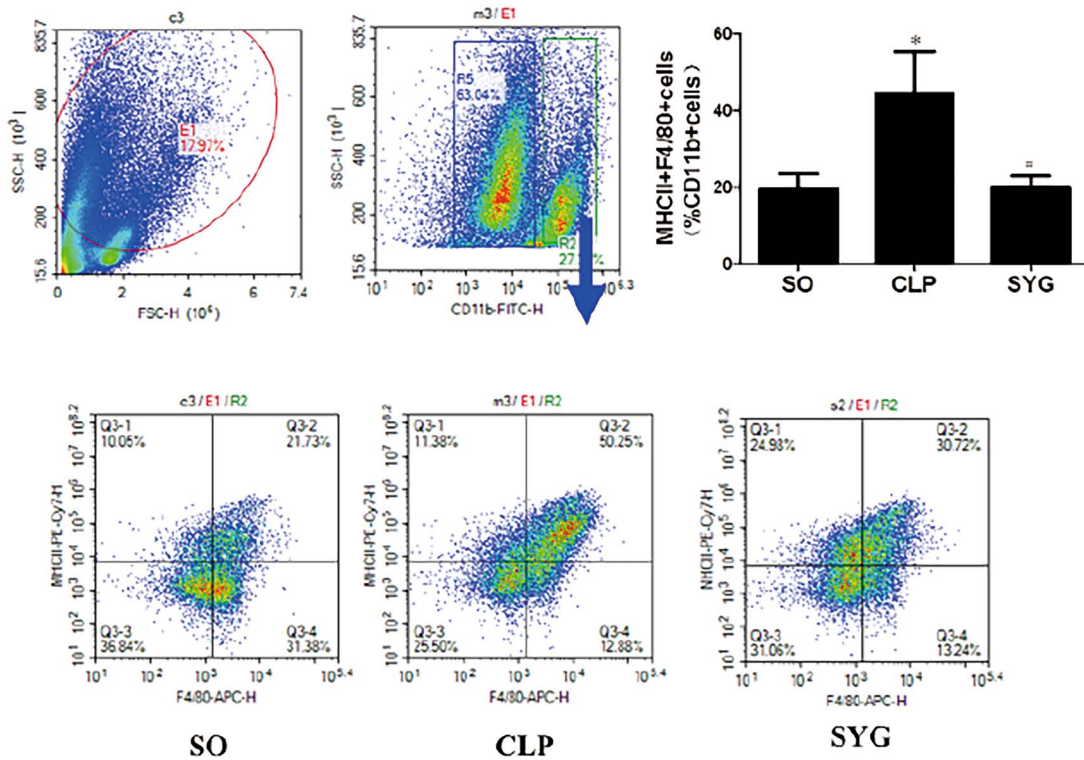
M1 macrophages in the Spleen

◄**Fig. 4** Effects of SYG on the polarization of macrophages to the M1 phenotype in BALF and sleep. Values are expressed as the mean ± *SD*. (*n* = 5 in each group) *$P < 0.05$ compared with the SO group; #$P < 0.05$ compared with the CLP group.

Effect of SYG on NLRP3 Inflammasome-Dependent Pyroptosis in LPS-Stimulated RAW 264.7 Macrophages

Our previous research found that SYG could decrease the mRNA levels of proinflammatory cytokines by suppressing the activation of Akt signalling pathways in LPS-induced RAW 264.7 macrophages [28]. However, it is unclear whether SYG inhibits NLRP3 inflammasome-dependent pyroptosis in macrophages. In this study, we treated RAW 264.7 cells with SYG before LPS + ATP and stimulation with the specific ERβ inhibitor PHTP. As Fig. 7 shows, SYG inhibits the activation of NF-κB signalling pathways (Fig. 7A) and reduces the protein expression of NLRP3, caspase-1 p20, ASC and Cle-Gasdermin D (Fig. 7B). In addition, real-time PCR assays also showed that

SYG decreased the mRNA levels of proinflammatory cytokines induced by LPS in RAW 264.7 cells (Fig. 7C), while the anti-inflammatory effects of SYG were abolished by ERβ inhibitors. These results suggested that SYG attenuated the inflammatory response in vitro by inhibiting NLRP3 inflammasome-dependent pyroptosis in LPS-stimulated RAW 264.7 macrophages.

DISCUSSION

Sepsis is defined as a dysregulated systemic response to infection that threatens the health and life of the population. Studies have shown that the lung is one of the most susceptible target organs in the development of sepsis, which further develops into ALI/ARDS [32]. In recent years, many natural polyphenolic compounds have been shown to exert anti-inflammatory and anti-oxidative stress properties, including SYG, which is present in many edible plant medicinal plants and is used in traditional Chinese medicine (TCM). In this study, SYG was isolated from *Sargentodoxa cuneata*, which exerts positive effects on
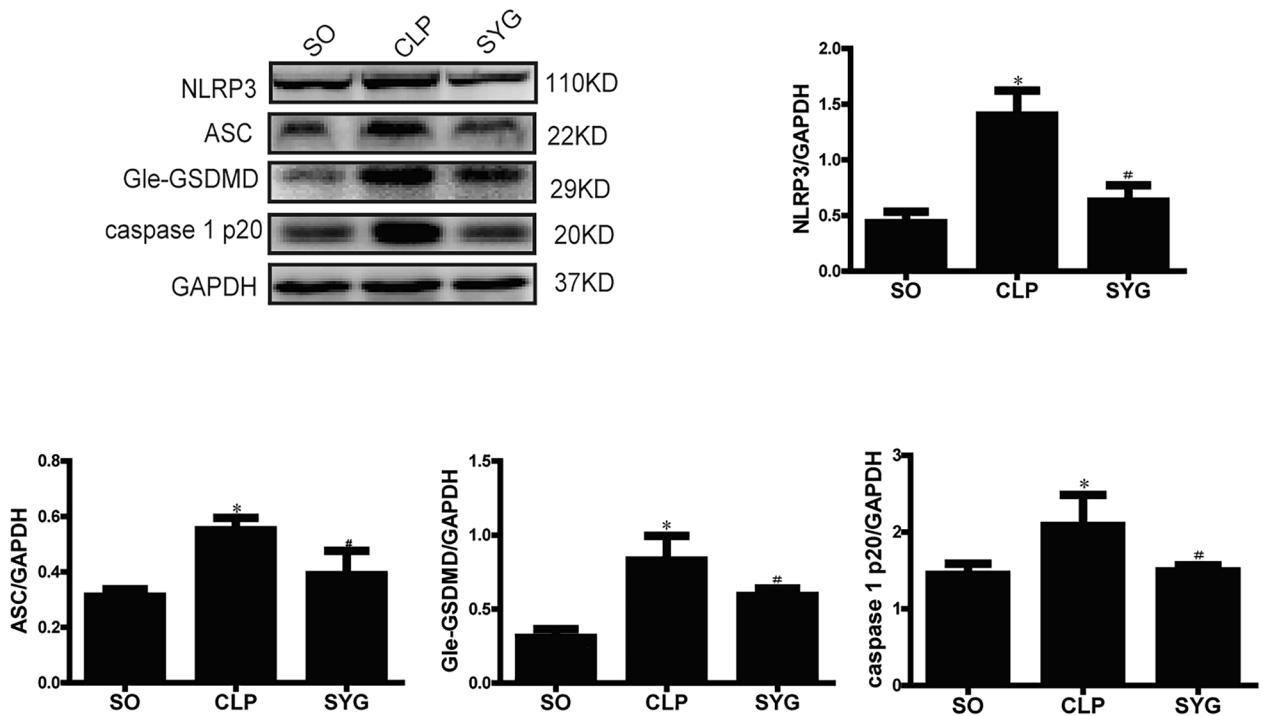

Fig. 5 Effect of SYG on NLRP3 inflammasome-dependent pyroptosis in mice with CLP-induced ALI. The protein expression of NLRP3, ASC, Cle-GSDMD and caspase-1 p20 in lung tissues. The values are expressed as the mean ± *SD*. (*n* = 5 in each group) *$P < 0.05$ compared with the SO group; #$P < 0.05$ compared with the CLP group.
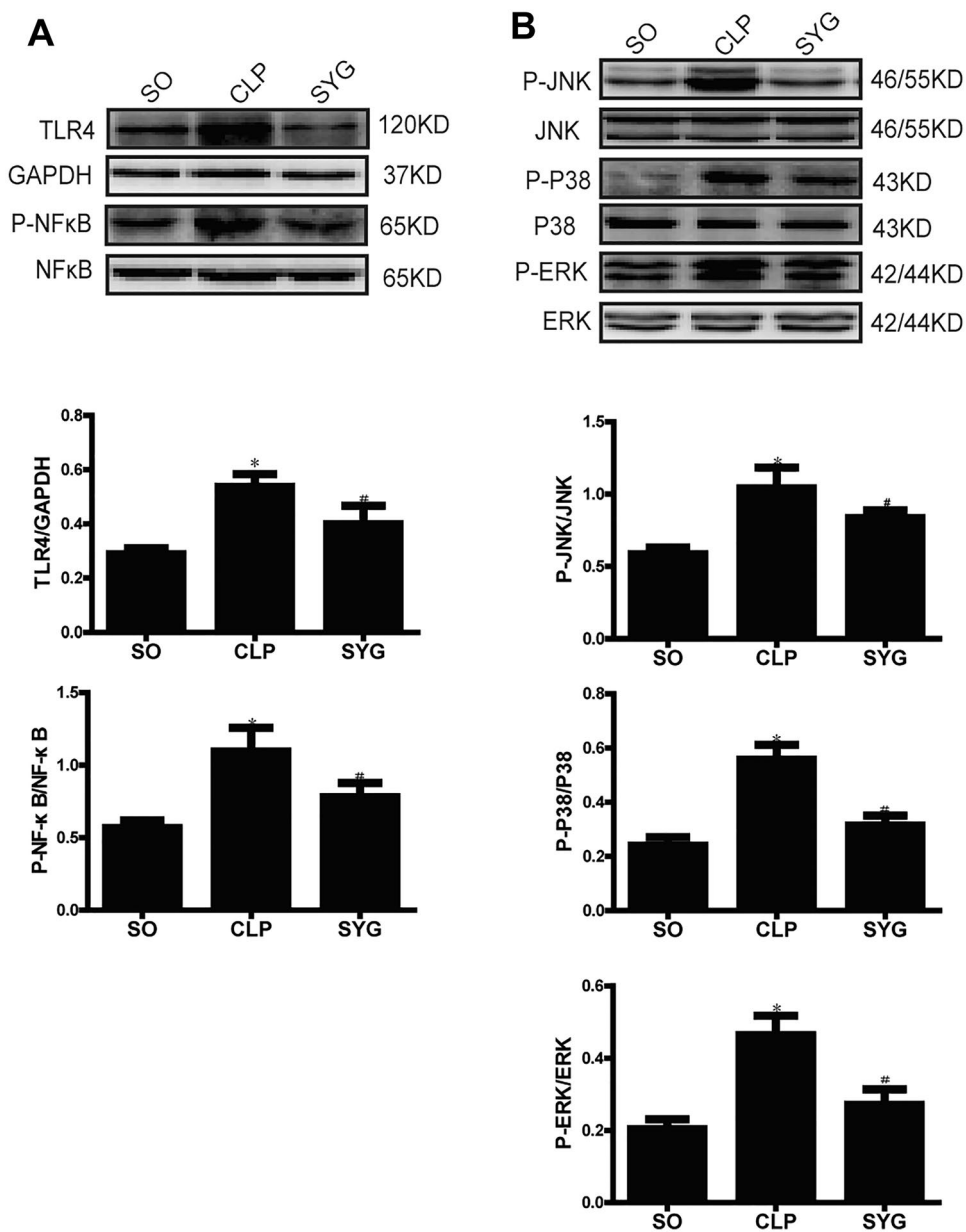
Fig. 6 Effect of SYG on TLR4/NF-κB/MAPK signalling pathway activation in mice with CLP-induced ALI. (**A**) The protein expression of p-NF-κB, NF-κB and TLR4 in lung tissues. (**B**) The protein expression of p-JNK, JNK, p-ERK, ERK, p-P38 and P38 in lung tissues. The values are expressed as the mean ± SD. ($n = 5$ in each group) *$P < 0.05$ compared with the SO group; #$P < 0.05$ compared with the CLP group.

inflammatory reactions and is used in many inflammatory diseases. We first investigated the potential protective effects of SYG against CLP-induced ALI in mice. ALI/ARDS is often associated with high mortality among patients in the ICU [33], and our results showed that SYG improved the survival rate of ALI mice for 7 days. Meanwhile, we found

that SYG alleviated lung tissue destruction and lung inflammation by decreasing the production of proinflammatory cytokines and inflammatory cell infiltration, along with improved pulmonary oedema in ALI mice.

Accumulating evidence indicates that uncontrolled and excessive inflammatory responses play a key role in
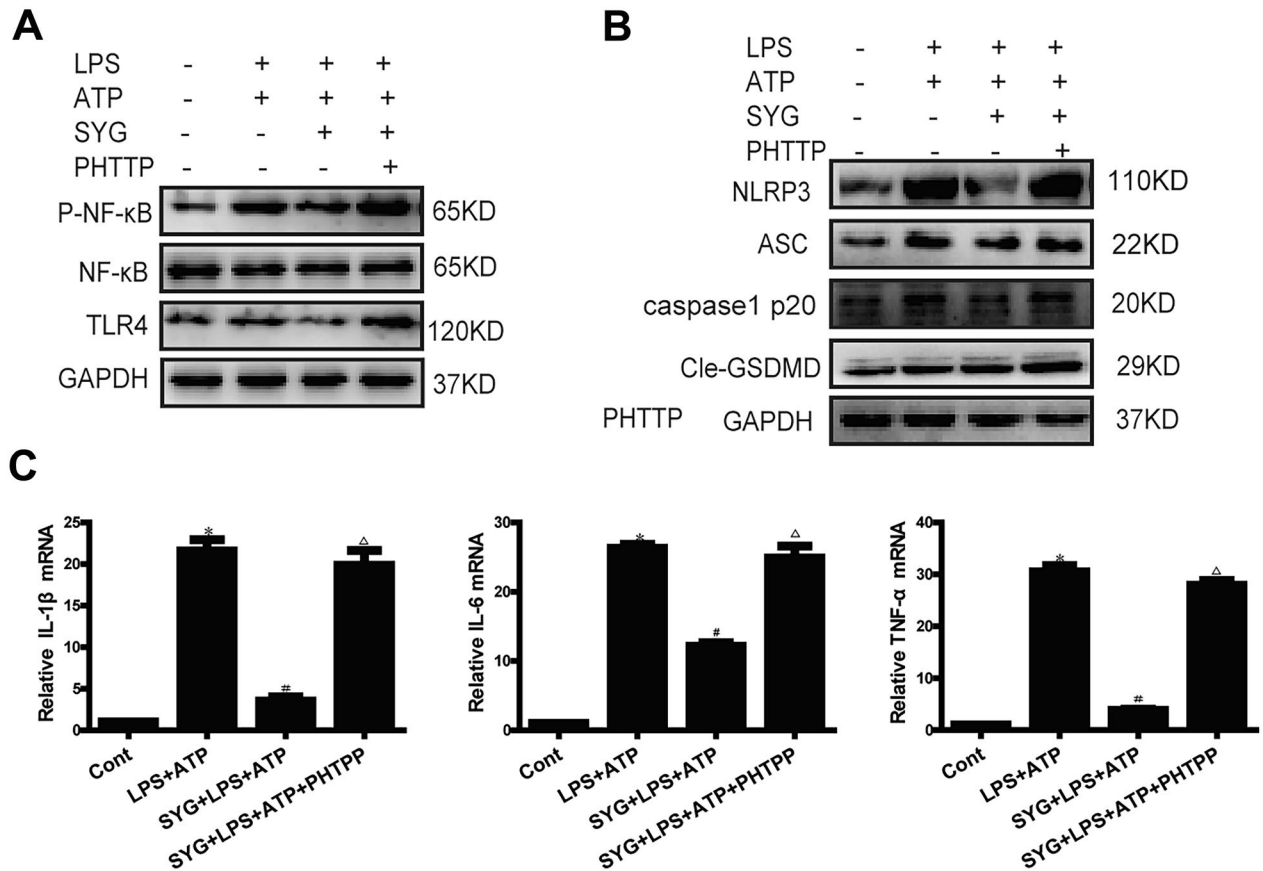
Fig. 7 Effect of SYG on NLRP3 inflammasome-dependent pyroptosis in LPS-stimulated RAW 264.7 macrophages. (**A**, **B**) The protein expression levels of NLRP3, ASC, caspase-1 p20, Cle-GSDMD, TLR4, NF-κB and p-NF-κB after ERβ antagonism (PHTTP). (**C**) The mRNA expression levels of TNF-α, IL-6 and IL-1β after ERβ antagonism (PHTTP). The values presented are the means ± SD. ($n = 3$ in each group) *$P < 0.05$ compared with the Cont group; #$P < 0.05$ compared with the LPS + ATP group; △$P < 0.05$ compared with the SYG + LPS + ATP group.

ALI, which contributes to the activation of macrophages and the accumulation of neutrophils in the lung [34]. These cells contribute to the pathogenesis of lung injury by mediating the excessive release of inflammatory cytokines and increasing the permeability of the alveolar capillary membrane [35]. To investigate the effect of SYG on pulmonary oedema, we detected the albumin content in BALF and found that the albumin content was significantly reduced after treatment with SYG in ALI mice. In addition, the activity of MPO in the BALF of ALI mice was increased, which is an indirect measure of neutrophils and reflects the degree of adhesion and migration of neutrophils in the lung tissues. After treatment with SYG, the MPO activity in lung tissue was markedly reduced compared with that in the SO group. Moreover, SYG dramatically decreased the levels of TNF-α, IL-6 and IL-1β in BALF and lung

tissues. Studies have demonstrated that macrophages play a pivotal role in the initiation and resolution of lung inflammation in ALI [36, 37] as the first barrier defending against pathogens in the lung, which are often described as two different phenotypes: classically activated macrophages (M1) and alternatively activated macrophages (M2). The balance between them is essential to control the excessive release of proinflammatory cytokines in ALI [38]. We found that SYG administration markedly suppressed the M1 macrophage phenotype in BALF and spleen.

NLRP3 inflammasome-dependent pyroptosis has been reported to be involved in the pathological process of ALI [39, 40]. The activated NLRP3 inflammasome participates in the occurrence and development of lung inflammation by inducing macrophage pyroptosis and releasing large amounts of proinflammatory cytokines such as IL-1β

and IL-18 [41, 42]. We found that NLRP3, ASC, Cle-GSDMD and caspase-1 p20 were significantly increased after CLP operation when compared to SO groups, while these effects were reversed by SYG administration. It has been reported that the activation of the NLRP3 inflammasome is mainly mediated by NF-κB and TLR4 [43]. In our present study, we found that CLP induced significant enhancement of the phosphorylation levels of NF-κB and TLR4 protein expression and that SYG pretreatment alleviated these effects of CLP in lung tissues. In addition, it has been reported that JNK, which is a member of the MAPK family, is involved in the activation of NLRP3 [44]. We detected the activation of the MAPK signalling pathway and found that the phosphorylation levels of JNK and p38 were decreased by SYG. These results implied that SYG suppressed the NLRP3 inflammasome in the priming step by inhibiting the activation of NF-κ, TLR4, JNK and p38 and then downregulated the expression of pyroptosis-related proteins, including NLRP3, ASC, Cle-GSDMD and caspase-1 p20, ultimately suppressing the release of the inflammatory cytokine IL-1β.

SYG is considered to be a phytoestrogen that possesses selective oestrogen receptor (ER)-modulating effects [45]. Previously, our reports showed that SYG exerts anti-inflammatory effects by suppressing the mRNA expression of proinflammatory cytokines and the Akt signalling pathway in RAW 264.7 cells treated with LPS, but the specific mechanism remains unclear. It has been reported that the upregulation of ER-β activity leads to inhibition of the NLRP3 inflammasome [46]. In this study, our results suggested that SYG could resist pyroptosis by inhibiting NLRP3 inflammasome activation in LPS- and ATP-treated RAW 264.7 cells, and this impact of SYG was abolished by the ERβ inhibitor PHTP. In addition, SYG also lowered the protein levels of TLR4, indicating that SYG attenuated NLRP3 inflammasome-dependent pyroptosis in vitro by inhibiting the expression of TLR4.

Although our results are encouraging, there are still limitations in the present work, and further studies are needed to clarify the precise molecular mechanism of the effects of SYG on ALI in vivo and in vitro. NLRP3 inflammasome activation is mediated by several signalling pathways. We focused on the oestrogen receptor-β signalling pathway in this study, and whether other signalling pathways are involved in the effect of SYG on the NLRP3 inflammasome and ALI is still not clear.

In conclusion, we propose for the first time that SYG reduces mortality and exerts protective effects in CLP-induced ALI. The mechanism of these protective effects could be that SYG inhibits the activation of the NLRP3 inflammasome by regulating the TLR4/NF-κB/MAPK signalling pathway, ultimately contributing to the therapeutic effects on ALI. These results suggest that SYG could be a potential therapeutic candidate for sepsis-induced ALI.

AUTHOR CONTRIBUTION

Jiarui Li and Ximo Wang designed this study. Yuzhen Zhuo and Lei Yang performed the experiment. Dihua Li analysed and interpreted the data, Lanqiu Zhang wrote the manuscript. Qi Zhang, Shukun Zhang, Caixia Li, Lihua Cui and Jian Hao participated in the experimental operation.

FUNDING

AVAILABILITY OF DATA AND MATERIAL

All the data generated or analysed during this study are included in this published article.

CODE AVAILABILITY

Not applicable.

Declarations

Ethics Approval and Consent to Participate Not applicable.

Consent for Publication All the authors agree to submit the final version of manuscript for publication.

Conflict of Interest The authors declare no competing interests.

REFERENCES

1. Ferguson, N.D., D.J. Cook, G.H. Guyatt, S. Mehta, L. Hand, and P. Austin, et al. 2013. High-frequency oscillation in early acute respiratory distress syndrome. *New England Journal of Medicine* 368 (9): 795–805.

2. Li, X.Y., J. Wang, H.S. Wu, P.P. Guo, C.Y. Wang, and Y.L. Wang, et al. 2018. Peripheral blood miR-140 may be a biomarker for acute lung injury by targeting Toll-like receptor 4 (TLR4). *Experimental and Therapeutic Medicine* 16 (4): 3632–3638.

3. Bellani, G., J.G. Laffey, T. Pham, E. Fan, L. Brochard, and A. Esteban, et al. 2016. Epidemiology, patterns of care, and mortality for patients with acute respiratory distress syndrome in intensive care units in 50 countries. *Journal of the American Medical Association* 315 (8): 788–800.

4. Mangia, C.M.F., N. Kissoon, J.A. Carcillo, et al. 2009. Sepsis and septic shock: A global overview. *Journal of Pediatric Infectious Diseases* 04 (02): 071–076.

5. Jiang, Z.L., A.L. Chen, L. Hu, L. Qiu, and L. Zhu. 2020. Calreticulin blockade attenuates murine acute lung injury by inducing polarization of M2 subtype macrophages. *Frontier Immunology* 30 (11): 11. https://doi.org/10.3389/fimmu.2020.00011.

6. Gao, W., Y. Wang, Y. Xiong, L. Sun, L. Wang, K. Wang, et al. 2019. Size-dependent anti-inflammatory activity of a peptide-gold nano-particle hybrid in vitro and in a mouse model of acute lung injury. *Acta Biomaterialia* 85: 203–217.

7. Li, D., W. Ren, Z. Jiang, and L. Zhu. 2018. Regulation of the NLRP3 inflammasome and macrophage pyroptosis by the p38 MAPK signaling pathway in a mouse model of acute lung injury. *Molecular Medicine Reports* 18 (5): 4399–4409. https://doi.org/10.3892/mmr.2018.9427.

8. Jorgensen, I., and E.A. Miao. 2015. Pyroptotic cell death defends against intracellular pathogens. *Immunological Reviews* 265 (1): 130–142.

9. Ying, Y.G., Y. Mao, and M. Yao. 2019. NLRP3 Inflammasome activation by microRNA-495 promoter methylation may contribute to the progression of acute lung injury. *Molecular Therapy-Nucleic Acids* Dec 6 801–814.

10. Lee, E.H., J.H. Shin, S.S. Kim, H. Lee, S.R. Yang, and S.R. Seo. 2019. *Laurus nobilis* leaf extract controls inflammation by suppressing NLRP3 inflammasome activation. *Journal of Cellular Physiology* 234 (5): 6854–6864.

11. Yang, H.H., J.X. Duan, S.K. Liu, J.B. Xiong, X.X. Guan, and W.J. Zhon, et al. 2020. A COX-2/sEH dual inhibitor PTUPB alleviates lipopolysaccharide-induced acute lung injury in mice by inhibiting NLRP3 inflammasome activation. *Theranostics* 10 (11): 4749–4761.

12. Lamkanfi, M., and V.M. Dixit. 2014. Mechanisms and functions of inflammasomes. *Cell* 157: 1013–1022.

13. Hooftman, Alexander, Stefano Angiari, Svenja Hester, Sarah E. Corcoran, and Marah C. Runtsch, et al. 2020. The immunomodulatory metabolite itaconate modifies NLRP3 and inhibits inflammasome activation. *Cell Metabolism* 32 (3): 468–478.

14. Shi, J., Y. Zhao, K. Wang, X. Shi, Y. Wang, H. Huang, Y. Zhuang, T. Cai, and F. Wang. 2015. Shao F Cleavage of GSDMD by inflammatory caspases determines pyroptotic cell death. *Nature* 526: 660–665.

15. Jo, E.K., J.K. Kim, D.M. Shin, and C. Sasakawa. 2016. Molecular mechanisms regulating NLRP3 inflammasome activation. *Cell Mol Immunol.* 13 (2): 148–59.

16. Shan, Q., G.H. Zheng, X.R. Han, X. Wen, S. Wang, and M.Q. Li. 2018. Troxerutin protects kidney tissue against BDE-47-induced inflammatory damage through CXCR4-TXNIP/NLRP3 signaling. *Oxidative Medicine and Cellular Longevity*, 9865495.

17. Zhong, W.J., H.H. Yang, X.X. Guan, J.B. Xiong, C.C. Sun, C.Y. Zhang, et al. 2019. Inhibition of glycolysis alleviates lipopolysaccharide-induced acute lung injury in a mouse model. *Journal of Cellular Physiology* 234 (4): 4641–4654.

18. He, X.Y., Z. Qian, E. Li, K. Fan, Y. Li, L. Wu, T.R. Billiar, M.A. Wilson, X. Shi, and J. Fan. TLR4-upregulated IL-1β and IL-1RI promote alveolar macrophage pyroptosis and lung inflammation through an autocrine mechanism. *Science Report* 6 (1): 1–11.

19. Dong, N., X. Xu, C. Xue, C. Wang, X. Li, C. Bi, and A. Shan. 2019. Ethyl pyruvate inhibits LPS induced IPEC-J2 inflammation and apoptosis through p38 and ER K1/2 pathways. *Cell Cycle* 18: 2614–2628.

20. Zhang, Z.Q., Q. Nian, C. Chen, A.Q. Cui, Y.Z. Han, and J.Y. Zhan. 2020. Klotho. Alleviates lung injury caused by paraquat via suppressing ROS/P38 MAPK-regulated inflammatory responses and apoptosis. *Oxidative Medicine and Cellular Longevity* 13 (2020): 1854206.

21. Altemimi, A., N. Lakhssassi, N. Baharlouei, D.G. Watson, and D.A. Lightfoot. 2017. Phytochemicals: extraction, isolation, and identification of bioactive compounds from plant extracts. *Plants* 6 (4): 42.

22. Habib, M., M. Trajkovic, and M.W. Fraaije. 2018. The biocatalytic synthesis of syringaresinol from 2,6-dimethoxy-4-allylphenol in One-Pot using a tailored oxidase/peroxidase system. *ACS Catalysis* 8 (6): 5549–5552.

23. Kim, J., T. Toda, K. Watanabe, S. Shibuya, Y. Ozawa, N. Izuo, and Cho, et al. 2019. Syringaresinol reverses age-related skin atrophy by suppressing FoxO3a-mediated matrix metalloproteinase -2 activation in copper/zinc superoxide dismutase-deficient mice. *The Journal of Investigative Dermatology* 139: 648–655.

24. Oh, J.H., Y.H. Joo, F. Karadeniz, J. Ko, C.S. Kong. 2020. Syringaresinol inhibits UVA-induced MMP-1 expression by suppression of MAPK/AP-1 signaling in HaCaT keratinocytes and human dermal fibroblasts. *International Journal of Molecular Science* 21(11): 3981.

25. Bajpai, V.K., M.B. Alam, K.T. Quan, M.K. Ju, R. Majumder, and S. Shukla, et al. 2018. Attenuation of inflammatory responses by (+)-syringaresinol via MAP-kinase-mediated suppression of NF-kappaB signaling in vitro and in vivo. *Science Reports* 8 (1): 9216.

26. Cho, Y.S., W.S. Song, S.H. Yoon, K.Y. Park, and M.H. Kim. 2018. *Syringaresinol suppresses excitatory synaptic transmission and picrotoxin-induced epileptic activity in the hippocampus through presynaptic mechanisms Neuropharmacology.* 131: 68–82.

27. Li, G.R., L. Yang, L.F. Feng, J.Yang, Y.F. Li, J. An, D.H. Li, et al. 2020. Syringaresinol protects against type 1 diabetic cardiomyopathy by alleviating inflammation responses, cardiac fibrosis and oxidative stress. *Molecular Nutrition & Food Research* 30: e2000231

28. Zhang, Z., L. Yang, B. Wang, L. Zhang, Q. Zhang, D. Li, S. Zhang, H. Gao, and X. Wang. 2017. Protective role of liriodendrin in mice with dextran sulphate sodium-induced ulcerative colitis. *International Immunopharmacology* 52: 203–210.

29. Zhuo, Y., S. Zhang, C. Li, L. Yang, H. Gao, and X. Wang. 2018. Resolvin D1 promotes SIRT1 expression to counteract the activation of STAT3 and NF-κB in mice with septic associated lung injury. *Inflammation* 41 (5): 1762–1771.

30. Hou, L.C., M.Z. Qin, L.N. Zheng, Y. Lu, D.R. Peng, X.P. Yu, Y.C. Xin, G.L. Ji, and L.Z. Xiong. 2009. Severity of sepsis is correlated with the elevation of serum high-mobility group box 1 in rats. *Chinese Medical Journal* 122 (4): 449–454.

31. Taratummarat, S., N. Sangphech, C.T.B. Vu, T. Palaga, T. Ondee, S. Surawut, A. Sereemaspun, P. Ritprajak, and A. Leelahavanichkul. 2018. Gold nanoparticles attenuates bacterial sepsis in cecal ligation and puncture mouse model through the induction of M2 macrophage polarization. *BMC Microbiology* 18 (1): 85.

32. Zhang, J., Y. Wang. Luo, X. Zhu, J. Li, Q. Feng, J., et al. 2019. Global transcriptional regulation of STAT3- and MYC-mediated sepsis-induced ARDS. *Therapeutic Advances in Respiratory Disease* 13: 1753466619879840.

33. Gao, W., Y. Wang, Y. Xiong, L. Sun, L. Wang, ang K. Wang, et al. 2019. Size-dependent anti-inflammatory activity of a peptide-gold nanoparticle hybrid in vitro and in a mouse model of acute lung injury. *Acta Biomaterilia* 85: 203–217.

34. Han, S., and R.K. Mallampalli. 2015. The acute respiratory distress syndrome: from mechanism to translation. *Journal of Immunology* 194 (3): 855–860.

35. Xia, W.F., Z. Pan, H.M. Zhang, Q.S. Zhou, and Y. Liu. 2020. Inhibition of ERR α aggravates sepsis-induced acute lung injury in rats via provoking inflammation and oxidative stress. *Oxidative Medicine Cellular Longevity* 2020: 2048632. https://doi.org/10.1155/2020/2048632.

36. Liu, M.Y., Y.L. Chen, S.Y. Wang, H.P. Zhou, D.Feng, and J. Wei, et al. 2020. α-Ketoglutarate modulates macrophage polarization through regulation of PPARγ transcription and mTORC1/p70S6K pathway to ameliorate ALI/ARDS. *Shock*. 53 (1): 103–113.

37. Yang, X.L., Y.B. Yin, X.X. Yan, Z.B. Yu, Y. Liu, and J. Cao. 2019. Flagellin attenuates experimental sepsis in a macrophage-dependent manner. *Critical Care* Apr 3 23 (1): 106.

38. Wang, N., H. Liang, and K. Zen. 2014. Molecular mechanisms that influence the macrophage m1–m2 polarization balance. *Frontiers in Immunology* 5: 614.

39. Ying, Y., Y. Mao, and M. Yao. 2019. NLRP3 inflammasome activation by microRNA-495 promoter methylation may contribute to the progression of acute lung injury. *Molecular Therapy Nucleic Acids* 18: 801–814. https://doi.org/10.1016/j.omtn.2019.08.028.

40. Peng, F., W. Chang, and Q Sun, et al. 2020. HGF alleviates septic endothelial injury by inhibiting pyroptosis via the mTOR signalling pathway. *Respiratory Research* 21 (1): 215. Published 2020 Aug 14. https://doi.org/10.1186/s12931-020-01480-3.

41. Youguo, Ying, Yong Mao, and Min Yao. 2019. NLRP3 inflammasome activation by microRNA-495 promoter methylation may contribute to the progression of acute lung injury. *Molecular Therapy-Nucleic Acids* Dec 6 18:801–814. https://doi.org/10.1016/j.omtn.2019.08.028.

42. Li, Dandan, Weiying Ren, and Zhilong Jiang. 2018. Regulation of the NLRP3 inflammasome and macrophage pyroptosis by the p38 MAPK signaling pathway in a mouse model of acute lung injury. *Molecular Medicine Reports* 18: 4399–4409.

43. Bauernfeind, F.G., G. Horvath, A. Stutz, E.S. Alnemri, K. MacDonald, D. Speert, T. Fernandes-Alnemri, J. Wu, et al. 2009. Cutting edge: NF-kappaB activating pattern recognition and cytokine receptors license NLRP3 inflammasome activation by regulating NLRP3 expression. *The Journal of Immunology* 183: 787–791.

44. Song, N., Z.S. Liu, W. Xue, Z.F. Bai, Q.Y. Wang, J. Dai, et al. 2017. NLRP3 phosphorylation is an essential priming event for inflammasome activation. *Molecular Cell* 68 (1): 185–197.

45. Heinonen, S., T. Nurmi, K. Liukkonen, K. Poutanen, K. Wähälä, T. Deyama, S. Nishibe, and H. Adlercreutz. 2001. In vitro metabolism of plant lignans: New precursors of mammalian lignans enterolactone andenterodiol. *Journal of Agriculture and Food Chemistry* 49 (7): 3178–3186.

46. Abdullaha, M., M. Ali, D. Kour, A. Kumar, and S.B. Bharate. 2020. Discovery of benzo [cd] indol-2-one and benzylidene-thiazolidine-2, 4-dione as new classes of NLRP3 inflammasome inhibitors via ER-β structure based virtual screening. *Bioorganic Chemistry* 95: 103500.